RESEARCH ARTICLE

Key Points:
- Archival records over the past 150 years show that the tidal amplitude has more than doubled in the upper Hudson River estuary
- Channel deepening for navigation reduced the effective friction, thereby amplifying the tide and storm surge along the estuary
- Channel deepening also increased conveyance of river discharge in the tidal river, such that the overall risk of flooding decreased

Correspondence to:
D. K. Ralston,
dralston@whoi.edu

Bigger Tides, Less Flooding: Effects of Dredging on Barotropic Dynamics in a Highly Modified Estuary

David K. Ralston[1] [iD], **Stefan Talke[2]** [iD], **W. Rockwell Geyer[1]** [iD], **Hussein A. M. Al-Zubaidi[2]** [iD], and **Christopher K. Sommerfield[3]** [iD]

[1]Woods Hole Oceanographic Institution, Woods Hole, MA, USA, [2]Portland State University, Portland, OR, USA, [3]University of Delaware, Lewes, DE, USA

Abstract Since the late nineteenth century, channel depths have more than doubled in parts of New York Harbor and the tidal Hudson River, wetlands have been reclaimed and navigational channels widened, and river flow has been regulated. To quantify the effects of these modifications, observations and numerical simulations using historical and modern bathymetry are used to analyze changes in the barotropic dynamics. Model results and water level records for Albany (1868 to present) and New York Harbor (1844 to present) recovered from archives show that the tidal amplitude has more than doubled near the head of tides, whereas increases in the lower estuary have been slight (<10%). Channel deepening has reduced the effective drag in the upper tidal river, shifting the system from hyposynchronous (tide decaying landward) to hypersynchronous (tide amplifying). Similarly, modeling shows that coastal storm effects propagate farther landward, with a 20% increase in amplitude for a major event. In contrast, the decrease in friction with channel deepening has lowered the tidally averaged water level during discharge events, more than compensating for increased surge amplitude. Combined with river regulation that reduced peak discharges, the overall risk of extreme water levels in the upper tidal river decreased after channel construction, reducing the water level for the 10-year recurrence interval event by almost 3 m. Mean water level decreased sharply with channel modifications around 1930, and subsequent decadal variability has depended both on river discharge and sea level rise. Channel construction has only slightly altered tidal and storm surge amplitudes in the lower estuary.

Plain Language Summary Dredging for navigation has deepened harbors and estuaries around the world, altering circulation patterns and tidal water levels. In the Hudson River estuary, channel construction for ports in New York Harbor and Albany more than doubled channel depths in some regions. Major dredging began in the late 1800s, so to characterize associated changes in the hydrodynamic conditions, we analyzed archival water level records and navigational charts back to that period. Water level records from Albany show that channel construction reduced the effects of friction such that the tide now amplifies in the upper estuary, more than doubling the tidal amplitude compared with before dredging. The lower friction also allows storm surge from the coast to travel farther landward. However, major flooding in the upper tidal river historically was mainly due to river discharge events, and the deeper channel allows for more effective conveyance of flood waves. Thus, despite the increases in tides and storm surge, the risk of flooding in the upper estuary decreased with construction of the navigational channel. The Hudson provides a well-documented example of how multiple anthropogenic factors can significantly influence physical processes in extensively modified estuaries.

1. Introduction

Estuaries and tidal rivers enable economic development by facilitating efficient maritime transportation and access to natural resources. Development of cities around estuaries has greatly modified their physical environment, including filling of intertidal and shallow subtidal waters, hardening of shorelines, and construction of navigational channels by dredging. These bathymetric alterations can significantly modify the hydrodynamics of an estuary, leading to changes in physical characteristics including the tidal amplitude, salinity distribution, stratification, and sediment transport. Altered physical processes can also impact estuarine ecosystems, for example, by changing residence times and nutrient retention, reducing the vertical exchange of oxygen (Talke et al., 2009), or altering wetland inundation (Jay et al., 2015). In many cases, these ecological impacts have detrimental consequences for the beneficial uses that initially spurred development around the estuary.

Isolating the effects of dredging on estuarine processes is challenging because individual deepening projects increase the depth by a small percentage and the morphological and ecological response time scales can be years to decades. Evaluation of estuarine conditions at the century time scale is often required to quantify significant changes due to bathymetric modification, but a paucity of quantitative data over this period is limiting in many systems (Talke & Jay, 2013). In the U.S., large-scale modifications of navigational channels began in the late nineteenth century (Familkhalili & Talke, 2016; Marmer, 1935) and has continued incrementally to the present (e.g., Chant et al., 2018). Many ports have planned or completed deepening projects to accommodate the larger container ships designed to pass through the expanded Panama Canal, including deepening projects to 50 ft (15 m) for the ports of New York and New Jersey, Baltimore, Norfolk, Charleston, and Miami, and to 45 ft (14 m) for numerous other U.S. ports. In many locations including New York Harbor, the controlling depth in the navigational channel has more than doubled since the late nineteenth century (Familkhalili & Talke, 2016).

Depth increases and maintenance dredging represent major perturbation to estuarine hydrodynamics, where shear stress at the bed is the major source of friction and is the source of turbulence and associated vertical mixing. Increases in water depth reduce the effects of bottom friction and reduce turbulent mixing of salinity or temperature stratification, potentially leading to changes in tidal processes, response to storm surge, the length of the salinity intrusion, and exchange with the coastal ocean. For tidal dynamics, a reduction in the effective drag due to deepening often corresponds with an increase in tidal amplitude and a change in phase with increased wave speed. Increases in tidal amplitude associated with dredging have been observed in many estuaries, including in the Thames (Amin, 1983), Rhine-Meuse (Vellinga et al., 2014), Elbe, Ems, and Loire (Winterwerp et al., 2013), Delaware (DiLorenzo et al., 1993), Columbia (Jay et al., 2011), Cape Fear River (Familkhalili & Talke, 2016), and Modaomen (Cai et al., 2012). Similarly, increased water levels during extreme events due to storm surge (Familkhalili & Talke, 2016) or river discharge (Vellinga et al., 2014) have been linked to bathymetric modification. The changes in the tide can be large, for example, with a doubling of tidal range in portions of the Delaware (DiLorenzo et al., 1993), the Ems (Talke & Jay, 2013), and Cape Fear estuaries (Familkhalili & Talke, 2016). Tidal range in the Garonne River of the Gironde Estuary has doubled due to gravel mining that increased depth and decreased roughness (Jalón-Rojas et al., 2018). In the Ems (de Jonge et al., 2014; Talke et al., 2009) and Loire (Jalón-Rojas et al., 2016), increases in tidal amplitude corresponded with a significant increases in suspended sediment concentration and landward shifts in the estuarine turbidity maxima. At high sediment concentrations fluid mud introduces a feedback that additionally reduces the effective drag on the flow, amplifies the tides, and leads to greater sediment trapping and a regime shift to hyperturbid conditions (Winterwerp, 2011). The balance of factors that control such regime shifts remains hard to predict or reproduce in realistic process-based models (Burchard et al., 2018).

The Hudson River adjacent to New York City provides an example of an estuary that has been significantly modified by the urbanization of its surrounding region, including infilling and hardening of the shoreline and dredging navigation channels (Chant et al., 2018; Panuzio, 1965). Previous research has built a solid understanding of the dynamics of the present-day estuary, but to understand how the system may have been modified by channel construction, we (a) recover, digitize, and analyze archival water level data back to the 1850s; (b) build and evaluate a retrospective numerical model using nineteenth century bathymetry; and (c) compare historical simulations with a validated numerical model of the modern estuary. Results from the observational and model analyses are framed with respect to theory for the barotropic dynamics, including an evaluation of the extent to which channel deepening by dredging in the Hudson has led to regime shifts in the tidal dynamics or response to extreme events.

2. Background

2.1. Hudson River Estuary

The Hudson River is a partially mixed estuary that discharges to New York Bight in the Atlantic Ocean (Figure 1), with New York City (NY, USA) located at its mouth. By convention and for comparison with previous studies, along-estuary distances in this study are referenced to The Battery at the southern tip of Manhattan, but the estuarine waters extend seaward another 25 km to the mouth of New York Harbor. Tides at the mouth have a mean range of about 1.5 m, and the influence of the tides extends 240 km landward of The Battery to
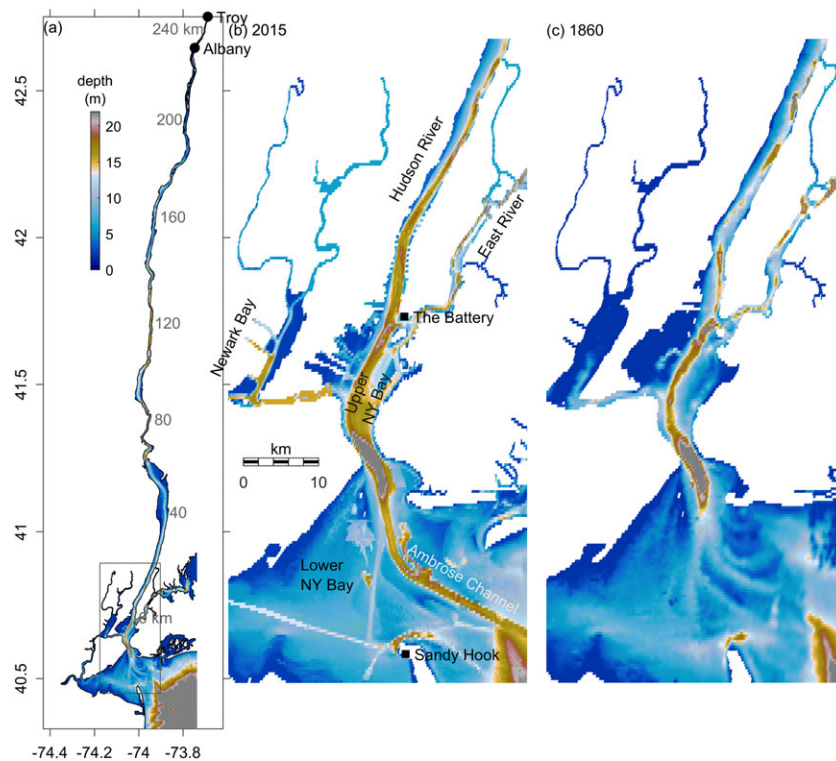
Figure 1. Hudson bathymetry. (a) Model domain, from New York Bight to the tidal limit of the Hudson River, (b) modern bathymetry in New York Harbor and the Lower Hudson Estuary, and (c) predredging (1860s) bathymetry in the same region.

the dam at Troy (NY). The Upper Hudson and Mohawk Rivers converge there to supply a mean annual discharge of about 400 m^3/s, and numerous smaller tributaries discharge directly to the tidal Hudson and increase the flow by 30%–40% (Wall et al., 2008). The salinity intrusion varies with river discharge and the spring-neap cycle of tides, typically extending landward from The Battery by 40–120 km (Abood, 1974; Bowen & Geyer, 2003; Ralston et al., 2008). Tidal influence extends landward of the salinity intrusion, a region Hoitink and Jay (2016) define as the tidal freshwater zone. Under high discharge conditions, the river input can modify the tide in the upper ~40 km of the Hudson such that the lowest water levels occur during neap rather than spring tides (Ralston & Geyer, 2018), which is the tidal river definition in Hoitink and Jay (2016).

The population of metropolitan area of New York City is currently more than 20 million, but human occupation of the region has been modifying the Hudson River estuary for centuries. Dutch settlers filled in marsh along lower Manhattan to create landings for commercial vessels, and this narrowing of the East River caused the adjacent Buttermilk Channel in Upper New York Bay to deepen from a few meters in the early 1700s to more than 12 m in 1807 (Steinberg, 2014). Active dredging to facilitate the growing ports in New York and New Jersey began in the late 1800s, when a 30-ft (9-m) channel was cut through the ebb-delta at the mouth of Lower New York Bay to allow passage of the newest class of steamships. Shortly thereafter, the Ambrose Channel was authorized (1899) and completed as a 40-ft (12-m) channel by 1914 (Steinberg, 2014). With the growth of the railroads the primary ports shifted from Brooklyn to Newark Bay (NJ), requiring dredging and maintenance of a navigational channel that is now 16-m deep in an embayment that had an average depth of 3 m prior to development (Chant et al., 2018).

In addition to the ports of New York and New Jersey in the lower estuary, a navigational channel with a minimum depth of 32 ft (10 m) is maintained to the Port of Albany, which is about 230 km upstream from New York Harbor and near the limit of tidal influence (Figure 2). Dredging of the upper Hudson began in the late 1860s with a 9–11-ft (3-m) channel, but the navigational channel was significantly
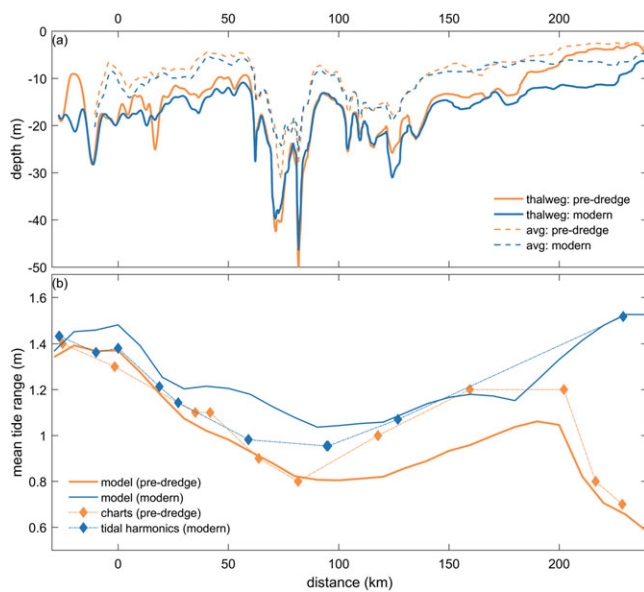
Figure 2. Along-channel depth and tidal amplitude. (a) Thalweg (solid lines) and average (dashed lines) depth from Ambrose Bar to the tidal limit in the Hudson River, comparing modern and historical conditions. (b) Mean tidal range along the same transect with model results (solid lines) and observations (square markers). Modern tidal ranges are from NOAA tidal prediction stations, and historical tidal ranges are from notations on historical charts.

deepened and widened in the late 1920s (Schureman, 1934). In addition to dredging, other major bathymetric alterations have occurred due to development along the estuary, including narrowing and deepening of the lower Hudson with expansion and hardening of the Manhattan shoreline (Klingbeil & Sommerfield, 2005) and infilling with dredge spoils of large areas of shallow subtidal in Upper New York Bay and the deep hole near the George Washington Bridge (18 km landward from The Battery; Panuzio, 1965).

The barotropic dynamics of the Hudson depend both on changing bathymetry in the estuary and on changes in the forcing from offshore. Near the mouth (Sandy Hook, NJ), the tidal range increased at a rate of 76 mm/century from 1932 to 2003, with similar trends at nearby stations (Flick et al., 2003). On the other hand, archival records show that the M_2 tide decreased at Sandy Hook and The Battery between the 1870s and 1930 (Talke et al., 2014). Storm surge events have increased in amplitude over the observational record in New York Harbor, with a 0.28-m increase in the level of the once-in-10-year event since 1856 on top of the 0.44-m increase in local sea level over that period (Talke et al., 2014). Notably, the storm surge of 3.4 m above mean sea level (MSL) due to Hurricane Sandy in 2012 was the largest since at least 1821 (Orton et al., 2016) and caused significant loss of life and damage to infrastructure in New York City. The causes of these storm surge changes remain uncertain. Here we assess how bathymetric modifications over a similar period may have influenced the magnitude of the tide, storm surge, and flood hazard along the estuary.

2.2. Methods and Data Sources
2.2.1. Bathymetry

Historical navigational charts for the Hudson River and New York Harbor were obtained from the Office of Coast Survey (https://historicalcharts.noaa.gov/) at the National Oceanographic and Atmospheric Administration (NOAA). A comprehensive, predredging bathymetry from the New York Bight to the head of tides in Troy (NY) was constructed from charts published between 1861 and 1870. The charts are based primarily on a hydrographic survey of the entire river in the summer of 1856 (and some measurements in 1858) and an associated leveling survey from 1856 to 1858. The tidal Hudson River is a glacially formed, relatively deep river in a narrow valley with limited floodplain. Predredging, the upper ~60 km of the tidal river likely had a more active floodplain with multiple shallow, braided channels around islands (Collins & Miller, 2012). The model does not account for wetting and drying of floodplain and instead focuses on the effects of changes in channel depth and width. Charts published from the 1860s to the present were obtained from the Office of Coast Survey to determine the changes in navigational channel depth through time. Charts for the upper tidal Hudson River (Coxsackie to Troy, currently chart #12348) and for Lower New York Bay (currently chart #12327) were used to determine the controlling depths for the navigational channel to Albany and for Ambrose Channel at the mouth of New York Harbor.

The modern bathymetry is compiled from multiple sources. In the Hudson and New York Harbor, the primary source was survey data collected between 1998 and 2004 by the Benthic Mapping Project by the New York State Department of Environmental Conservation. In Lower New York Bay the primary sources were digital elevation models from NOAA's National Center for Environmental Information and the Federal Emergency Management Agency's Region 2 coastal storm surge model. Bathymetric survey data collected for the U.S. Army Corps of Engineers after the deepening of the major navigational channels of New York Harbor and Newark Bay was completed (2013–2014) were also incorporated into the modern bathymetry.

2.2.2. Observed Water Level and Discharge

Water level observations back to the midnineteenth century were compiled from multiple sources to produce tidal records that span the length of the tidal Hudson from the Atlantic Ocean to the head of tides. In New York Harbor hourly tide records (1860 to present) and high/low tide records (1844 to present) were compiled (Talke et al., 2014), including tide records from The Battery (NOAA #8518750; 1920–1921, 1927 to present) and Sandy Hook (NJ) (#8531680, 1910–1918, 1932 to present) and recently digitized tide records from the U.S. National Archives including Governors Island (1844–1879; 1885; located 2 km from The Battery), Fort Hamilton (1893–1930, located 15 km seaward of The Battery), and Sandy Hook (1855–1857 and 1875–1893). Additional information on historical measurement techniques and data, as well as quality assurance methods, is provided by Talke and Jay (2013, 2017).

Water level records from Albany (NY) near the limit of tidal influence were digitized from multiple sources spanning the period from 1868 to present. Pictures of twice daily High/Low Water tabulations for 1868, 1875–76, 1894–1899, 1906–1909, and 1914–1939 were made from paper records of the United States Army Corps of Engineers (USACE) at the Federal Records Center in Lee's Summit, MO, and additional USACE records for 1899–1904 and 1914–1940 were found in Coast and Geodetic Survey records at the U.S. National Archives in College Park, MD. A copy of these records was found in the EV2 database at the National Center for Environmental Information, along with a superseded station summary, tabulations of extremes, and other documents associated with the Schureman (1934) report. High/Low records from 1943 to 1982 were obtained from the regional USACE office in Albany, NY. The High/Low records were digitized into spreadsheets along with hourly records for 1903, 1904, 1914, 1922, 1928, 1934, and 1940. Quality assurance was applied as described by Talke and Jay (2017).

The archival USACE measurements from Albany (1868–1982) were combined with modern digital records to produce a partial tide record from 1868 to 1913 and a nearly continuous record from 1914 to 2017. Hourly tide records were obtained from NOAA (#8518995) from October 1981 to July 1987, and unpublished digital tide records were obtained from the U.S. Geological Survey (USGS, #01359139) at 15-min resolution for the period October 1983 to March 2002. Officially verified High/Low data were obtained from the USGS for 1999–2017, along with additional 15-min resolution data since 2002.

Tide records were reduced to the National Geodetic Vertical Datum of 1929 (NGVD-29), the datum for the USGS records. For 1914–1950 and 1951–1972, USACE tabulations were referenced to a datum 2 and 2.09 ft, respectively, below NGVD-29. Perhaps reflecting a gauge change, the offsets to NGVD-29 between 1973–1975 and 1976–1982 were noted as 10 and 0 ft, respectively. Measurements from 1868 to 1914 were tabulated relative to a local datum (anywhere from 75 to 80 ft below the staff zero) but were also referred to the *Gristmill benchmark* at the ferry dock in Greenbush (NY), across the river from Albany. The Gristmill benchmark, cut into a stone cellar in 1857 by the U.S. Coast Survey, was described as 13.86 ft above the sea level datum (i.e., NGVD-29) in archival documents dated between 1910 and 1932, allowing the USACE data from 1868 to 1982 to be converted to NGVD-29 based on the staff zero relative to the Gristmill benchmark.

The USACE data in NGVD-29 were combined with modern USGS and NOAA data, using periods of overlap between the sources used to ensure datum consistency. The USGS datum was 10 ft below NGVD-29 from 1983 to 2002 and 0 ft offset for 2002 to present, and the NOAA datum was 9.91 ft below NGVD from 1981 to 1987. Based on comparisons between data sets, we assign an uncertainty of 0.03 m to the datum from 1914 to present, noting that (a) it is unclear why a 0.09-ft datum shift (0.027 m) occurred in USACE data in the 1950s or exactly when it occurred and (b) it is unclear whether NOAA, USGS, and USACE maintained separate gauges in the 1980s or reported the same data relative to a slightly different datum. Earlier measurements may have somewhat larger datum error, due to lack of documentation and discrepancies in the estimate of the Gristmill benchmark height relative to mean sea level at Sandy Hook from 1876 to 1882. However, our estimates of mean tide level agree well with the Schureman (1934) compilations and are consistent with expectations for the effect of dredging (see section 3). Therefore, we conclude that any datum errors are slight relative to the observed changes in mean tide level over time.

We use the Albany (1868–2017) water level data to obtain a record of the 400 largest recorded events, as well as a time series of the annual maximum water level. Data are filtered such that the gap between successive events is at least 6 days, to avoid double counting individual storm events. Nonetheless, it is likely that many

extreme events before 1914 were missed because tide records were only collected during nonwinter (ice-free) periods, typically between March/April and October/November. Fortunately, high water marks were tabulated both in Coast and Geodetic Survey records and in Schureman (1934), enabling a nearly continuous record of annual extreme water levels for 1893 to the present. Water levels during extreme freshets back to 1839 were also documented in Schureman (1934), allowing comparison between nineteenth century and modern extremes.

A generalized Pareto Distribution (GPD; Kotz & Nadarajah, 2000) was used to evaluate the flood hazard from 1893 to 1929 (i.e., before major dredging in the upper river) and the modern flood hazard since 1960. Such a peak-over threshold analysis allows inclusion of multiple events from a single year. By only analyzing the tail of the extreme value distribution, the GPD analysis also deals with gaps in the record in which it is known that no large freshets over the chosen threshold occurred (e.g., 1911–1912). Due to a large downward shift in extreme water levels (see section 3), different thresholds were required for different periods. Prior to 1930, only water level data greater than 3.5 m above NGVD-29 were used; after 1960, a smaller threshold of 2.5 m was applied. These thresholds were selected to represent the tails of the probability distributions and yet retain enough data to minimize uncertainty. Parameters in the fit were obtained using a Maximum Likelihood Estimate (MLE) method in MATLAB. Parameter confidence intervals from the MLE were used to generate parameter distributions that were then randomly sampled in a Monte Carlo approach to generate a suite of recurrence interval curves ($n = 10^4$). Confidence intervals shown for the recurrence interval curves were based on this Monte Carlo sampling.

Along with the detailed water level time series from near the mouth and head of tides, we use tidal range estimates based on shorter-term records at multiple locations to evaluate changes along the estuary. Charts from the 1860s included notation on tidal ranges at several locations (Sandy Hook, NJ; Governor's Island, Dobb's Ferry, Tarrytown, Verplank's Point, West Point, Poughkeepsie, Tivoli, Stuyvesant, Castleton, and Albany, NY), and these were used for comparison with the predredging model results. These tide range estimates were confirmed using the original, short-period tide records used for the bathymetry survey of 1856–1858 and recovered from the U.S. National Archives. For modern conditions, we use NOAA tidal predictions along the estuary for harmonic stations (Sandy Hook, NJ; USCG Station, The Battery, Dyckman Street, Haverstraw Bay, Beacon, Hyde Park, and Albany, NY) and subordinate stations (Alpine, NJ; Peekskill, Poughkeepsie, Kingston, Tivoli, and Castleton, NY).

The largest tributaries discharging into the tidal Hudson are the Upper Hudson and Mohawk Rivers, which converge just upstream of the head of tides. USGS gauging records on the Upper Hudson at Waterford (#01335754) are available from 1887 to present and on the Mohawk at Cohoes (#01357500) from 1917 to present. The Green Island gauge (#01358000) is downstream of the convergence and operated seasonally back to 1946. A combined observational time series of discharge is created from these sources for the period 1917–2017. To estimate discharge in the Mohawk for 1887–1917, we use observations from Waterford and multiply by the slope of the regression (0.78) between the Upper Hudson and Mohawk during the period of overlapping observations. This is similar to the ratio (0.75) of the long-term average discharges for the Upper Hudson (224 m³/s) and Mohawk (167 m³/s).

In addition to the modifications by dredging, conditions in the Hudson have been modified by changes in the fluvial inputs due to dams built for flow regulation. One of the largest flow control structures in the watershed is the Conklingville Dam, which was built on the fluvial Upper Hudson River more than 100 km upstream of Albany in response to a discharge event and severe flooding that occurred in March 1913. The dam became operational in 1930, approximately the same time that the upper tidal river was significantly deepened. To assess the effects of flow regulation on the discharge regime, we calculate recurrence intervals based on observations of annual maximum discharge on the Upper Hudson at Waterford before and after the dam came online. The recurrence intervals are based on a Generalized Extreme Value distribution fit (Kotz & Nadarajah, 2000), similar to the GPD fit used for water level. Confidence intervals are calculated using the parameter fit uncertainty from the MLE and Monte Carlo sampling, as above.

2.2.3. Hydrodynamic Model

A numerical model of the Hudson River and surrounding region that has previously been developed and evaluated against observations was adapted to assess effects of changes in bathymetry since the 1800s. The model uses the Regional Ocean Modeling System (Haidvogel et al., 2008; Warner et al., 2010), and the
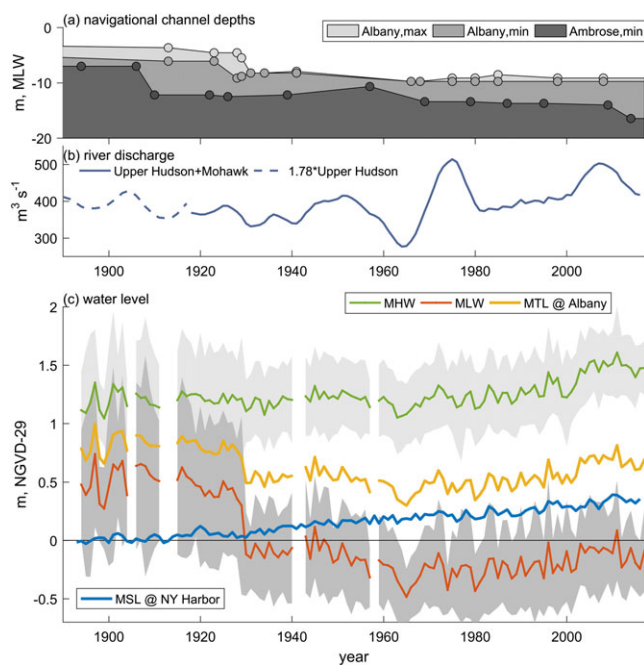
Figure 3. Channel depth and observed water level. (a) Controlling depth from navigational charts for the Hudson River south of Albany and for Ambrose Channel in Lower New York Bay. Markers indicate hydrographic survey dates reported on charts. (b) Mean (5-year moving average) river discharge at Albany from observations of the Mohawk and Upper Hudson River (1918–2016) or observations of the Upper Hudson (1888–1917) scaled by a factor (1.78) to reflect the average flow from the Mohawk. (c) Time series of mean high water (HW) and mean low water (MLW) at Albany. Solid lines are annual averages of daily observations, and gray shading is plus/minus one standard deviation. Also shown are and mean tide level (MTL) at Albany and mean sea level (MSL) in New York Harbor (Fort Hamilton before 1920 and The Battery since 1920).

domain extends from New York Bight to the tidal limit of the Hudson including New York Harbor and its principal subembayments (Figure 1). Grid resolution is 100 to 500 m in the along-channel direction and 20–60 m across channel and consists of 16 evenly distributed sigma layers in the vertical. Water level open boundary conditions are applied in Western Long Island Sound and in New York Bight using nine tidal constituents plus observed low-pass-filtered water levels from NOAA stations at Sandy Hook, NJ, and Kings Point, NY. Observed river discharge is input from the Upper Hudson and Mohawk Rivers and 10 smaller tributaries that flow into the tidal Hudson and the lower bays.

The circulation model is run using the two bathymetric configurations: predredging bathymetry based on the 1860s era charts and modern bathymetry (Figures 1 and 2). The model grid and forcing configuration is the same for both cases, and only the bathymetry is changed. Idealized, constant discharge scenarios were run with simplified tidal forcing (M_2, S_2, and N_2 components) to represent spring-neap variability for a range of discharge conditions: 150, 300, 600, 2,000, and 5,000 m^3/s (Ralston & Geyer, 2018). Constant discharge simulations were run until reaching periodic equilibrium with the tidal variability, up to 6 months for the low discharge cases. The idealized forcing cases are used here to quantify changes in the tides and river slope over the typical range of discharge conditions. Realistic forcing simulations also were run for Tropical Storms Irene and Lee in 2011 (Ralston et al., 2013) and Hurricane Sandy in 2012. Those realistic simulations are used to examine the response of the estuary to major discharge events and storm surge.

To evaluate the effects of changing bathymetry, the constant discharge and realistic forcing cases were run with the predredging bathymetry. Model boundary conditions, bottom roughness, and grid discretization were the same as for the modern bathymetry cases, such that intermodel comparisons reflect only the effect of bathymetric changes. Note that the simulations were run without wetting and drying, and shallow regions were set to have a minimum depth of 2 m relative to MSL. The Hudson has limited intertidal area, but under high river discharge the inundation of floodplains of the upper tidal river may be underestimated. Bottom roughness height (z_0) was set uniformly equal to 5 mm based on previous calibrations of the modern model (Ralston et al., 2012).

3. Results and Interpretation

3.1. Tidal Amplitude

The water level record at Albany shows a continual change in annually averaged mean high water (MHW) and mean low water (MLW) since the nineteenth century, reflecting both changes in tidal range and mean water level (Figure 3). Since the 1860s, tidal range increased from about 0.6 to 1.6 m due both to increases in MHW and decreases in MLW, with the biggest change occurring around 1930 (Figure 3c). Similarly, the annual average MLW decreased rapidly from 0.6 to −0.1-m NGVD29 around 1930. MHW remained relatively steady over the first century of the record and then increased from about 1.2 to 1.5 m starting in the 1960s. The change in tidal range reflects the combined MHW and MLW changes (Figure 3c). However, the decrease in MLW elevation (~0.7 m) was much greater than the increase in MHW (~0.3 m). Observations in the Columbia River found a similar discrepancy between low and high water responses to channel deepening, with decreased MLW of 0.4–0.5 m under low discharge conditions and only small changes in MHW (Jay et al., 2011). The decrease in MLW reflects the additive effects of increased tidal range and decreased mean water level associated with the river discharge, as shown below, whereas the two effects nearly offset to make for smaller changes in MHW. Interannual variations in sea level at the coast also affect water level in Albany, as detailed below.

The sharp decrease in MLW coincided with the deepening of the navigational channel to Albany in the late 1920s (Figure 3a). Prior to modification, this region was a shallow, braided river with multiple channels flowing around numerous islands, and dredging converted it to a deeper, single-threaded channel (Collins & Miller, 2012). In bathymetric surveys in 1928 and 1929, thalweg depths in the upper 60 km of the river ranged from 4.5 to 9.1 m, compared with thalweg depths of 3.7 to 6.1 m in 1913. By 1931 the controlling depth along the entire upper 40 km of the river was 8.2 m, as found in a 1941 survey. Additional dredging increased the controlling depth to 9.8 m between 1941 and 1966, which corresponded with a further 0.3-m decrease in MLW. The maximum depth was maintained at 9.8 m through 2008, although some sections of the channel were slightly shallower (8.5–9.3 m) based on surveys from 1975 and after. Collectively, the bathymetric modifications in the upper river have increased the thalweg and average depths by a factor of about 2.5 (Figure 2a), and large areas of shoals and secondary channels have been filled by dredge spoils. The timing of the changes in the navigational channel are concordant with the changes in the tides at Albany, where there was a major decrease in MLW at the initial dredging in the late 1920s (Figure 3c). Another factor potentially affecting the tides in the upper river is construction of the Federal Dam at Troy in 1915, built to improve navigation in the fluvial river upstream. The river was shallow and sinuous in this region prior to dam construction, and near the limit of tidal influence. No obvious change in Albany tide MLW, MHW, or tide range is observed around 1915, suggesting no immediate effect of dam construction at that location (Figure 3c). However, deepening in the late 1920s may have allowed wave reflection and contributed to the increase in tide range, similar to reflection off a weir and increased tidal amplitude in the Ems River Estuary (Talke & Jay, 2013).

Both MLW and MHW have increased steadily since about 1965 and in part due to sea level rise at the coast. The rate of increase of mean water level at Albany over this period was 5.4 ± 1.4 mm/yr, about 50% greater than the rate of sea level rise at The Battery of 3.3 ± 0.7 mm/yr over the same period (Figure 3c). However, the rate of change of mean water level at Albany varies more at decadal time scales than at The Battery. Over the period since 1945, the average rate of increase at Albany was 2.7 ± 1.1 mm/yr, compared with 3.0 ± 0.4 mm/yr at The Battery over the same period. As examined in greater detail in the next section, both mean and tidal water level in the upper tidal river depend not only on the forcing from the seaward boundary but also the river discharge, which varies at decadal time scales (Figure 3b). The 1960s were a period of drought in the Hudson watershed and corresponded with decreased mean water levels, whereas recent decades have been comparatively wet and resulted in higher average water levels. Long-term variations in tidal and mean water level at Albany therefore reflect both climatic forcing factors, like sea level rise and precipitation trends, and anthropogenic modifications like channel construction and discharge regulation.

We assess the spatial pattern of changing tides using the sparse historical measurements between The Battery and Albany and the numerical simulations (Figure 2b). Historical measurements suggest that tidal range decreased from about 1.4 m near the mouth to 0.8 m at 80 km (West Point), increased to about 1.2 m from 150 km (Tivoli) to 200 km (Stuyvesant), and decreased thereafter to 0.7 m at 230 km (Albany). Model results with predredging bathymetry demonstrate similar along-estuary variability in tidal amplitude, with a local minimum around 100 km, an amplification to about 200 km, and a sharp decrease landward to the head of tides. In contrast, mean tidal ranges according to both modern NOAA harmonics and the model with modern bathymetry continue to increase in the upper 40 km, reaching an amplitude greater than at the mouth (Figure 2b). The greatest differences between the predredging and modern bathymetry model results are in the upper tidal river, and the modeled increase in the tidal range at Albany from 0.7 to 1.6 m is consistent with the water level time series (Figure 3c). The modeled tidal amplitude in the Harbor and lower estuary is slightly greater with the modern bathymetry than predredging, but the increase is less than 10%.

In the upper 40 km of the Hudson, average channel depth has increased by a factor of 2.5 since 1860, while the modeled tidal range increased by a factor of 2.2 (Figure 2b). While dredging has increased the depth of the main channel, dredge spoil disposal greatly reduced the extent of secondary channels and shoals (Collins & Miller, 2012). According to theory, both deepening and the narrowing would increase tidal amplitude in a frictional estuary (Friedrichs, 2010; Friedrichs & Aubrey, 1994; Jay, 1991). In a convergent estuary, frictional damping tends to reduce the tidal amplitude, while width convergence
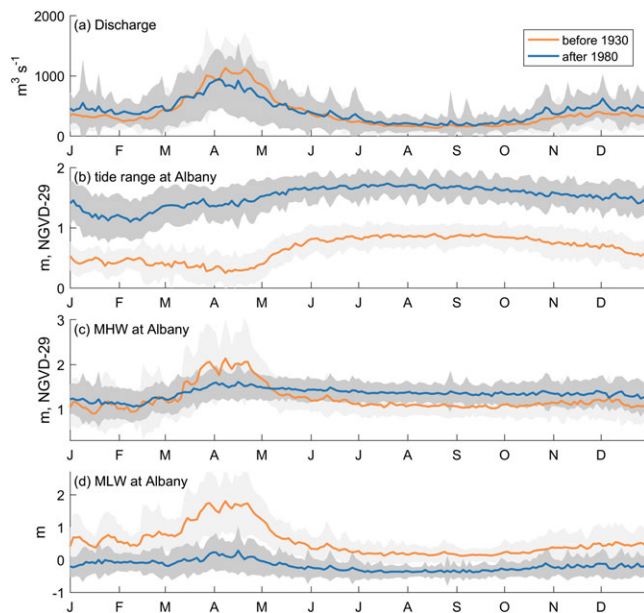
Figure 4. Observed river discharge and water level at Albany. (a) Annual variation in river discharge at Albany (Mohawk River + Upper Hudson River), with daily averages for the periods before 1930 and after 1980. Gray shading is plus/minus one standard deviation. (b) Annual variation in mean tidel range at Albany. (c) Annual variation in mean high water. (d) Annual variation in mean low water.

has the opposite effect. To evaluate the relative strengths of these competing effects, the exponential convergence length scale (L_w) can be compared with the frictional length scale (c/r), where $c = \omega/k$ is the tidal wave speed, equal to the tidal frequency ω divided by the wave number k, and r is a linearized friction factor. Considering only the dominant M_2 constituent, the linearized friction factor incorporates the tidal velocity amplitude U and the tidally averaged depth H as follows:

$$r = \frac{8}{3\pi} \frac{C_d U}{H} \tag{1}$$

where C_d is the drag coefficient (Friedrichs & Aubrey, 1994). If L_w is much less than c/r, then the tide is amplified due to tidal energy flux convergence, whereas if c/r is much less than L_w, then the tide decays exponentially due to friction. Convergence in depth can also amplify the tide, but dredging has reduced the depth convergence (or increased the depth convergence length scale) in the upper tidal Hudson, which would have the opposite effect on the tides than was observed.

We calculate the convergence length scale as $L_w = W/(\partial W/\partial x)$, where W is the channel width and x is the along-river distance. The friction factor is calculated assuming $C_d = 3 \times 10^{-3}$, $U = 0.7$ m/s, and the thalweg depth for H. The shallow water wave speed is $\sqrt{gH}$. Note that the shallow water speed is slightly modified by friction, which we ignore to first order (Jay, 1991). Comparing the predredging and modern bathymetries, changes in channel width increased L_w only slightly. Averaged over the upper tidal river (>180 km), L_w was 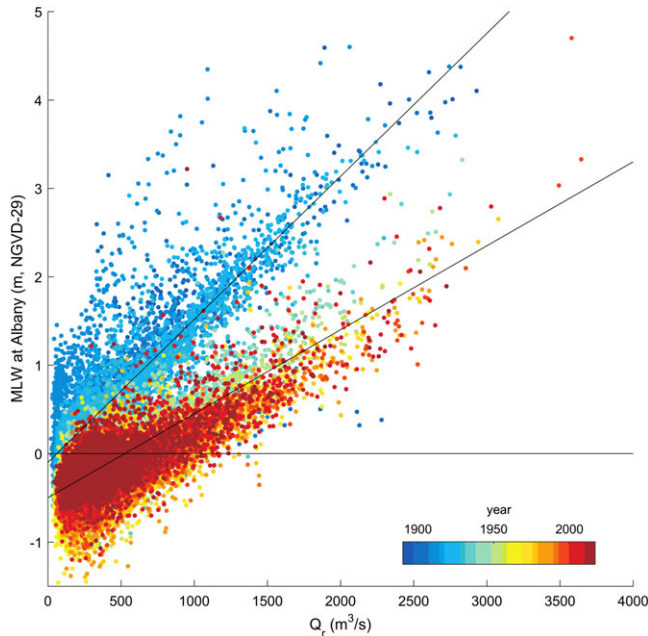58 km for the predredging bathymetry and 61 km for the modern bathymetry. In contrast, the increase in average channel depth in this region more than doubled the average c/r, from 28 to 71 km. Greater intertidal area in the predredging conditions would suggest an even lower value for c/r.

Prior to dredging $c/r < L_w$, which is consistent with the observed frictional damping of the tide in this region and is termed hyposynchronous (Nichols & Biggs, 1985). In the modern estuary, the opposite condition holds and $L_w < c/r$. Hence, convergence amplifies the tide and the estuary is termed hypersynchronous. In addition to the depth change, dredging tends to reduce the effective roughness of the channel by removing sand waves and reducing channel sinuosity (Jay et al., 2011). Hardening of the banks and loss of wetland cover might also reduce the effective friction. These changes in channel roughness would reduce the effective C_d and also lead to increased tidal amplitude. Note that the model did not incorporate any changes in bottom roughness or intertidal area that might be associated with dredging, so the simulations reflect primarily the decrease in effective drag due to increased depth.

In contrast to the secular changes in tides in the upper estuary, the effects of dredging on tides in the lower estuary have been small. The modeled tidal range at The Battery increased by 0.1 m (7%) between predredging and modern conditions, and the M_2 amplitude increased by 0.04 m (7%), similar to the 0.03 m (5%) increase in the measured M_2 since the 1920s (Talke et al., 2014). Hence, the channel deepening in New York Harbor accounted for roughly 5% of the observed increase in tidal range in Albany. Prior to major dredging operations, tidal amplitude in the lower estuary actually decreased slightly, as measurements at both Sandy Hook and Governors Island indicate that M_2 decreased by 0.02 to 0.03 m between 1860 and 1920 (Talke et al., 2014). Since deepening in the estuary slightly increased tidal amplitudes, the model results suggest that the late nineteenth century decrease was caused by altered oceanic tidal conditions.

3.2. Water Level Dependence on River Discharge

Seasonal changes in the hydrograph in the upper Hudson River over the past century have been consistent with a shift toward a more rain-fed-, rather than snowmelt, driven system (Hayhoe et al., 2007; Figure 4a). The average flow from October to February has increased by 34%, from 311 to 418 m³/s, while the magnitude of the snowmelt-driven spring freshet from mid-March to mid-May has decreased by 17%. On an annualized

Figure 5. Observed daily mean low water (MLW) at Albany versus river discharge (Q_r). Data are colored according to date shown in colorbar. Reference lines differ by a factor of 1.7, the ratio of the average depths in the modern and historical bathymetry landward of 180 km (6.3 and 3.7 m, respectively).

basis the changes are smaller, with the mean discharge for the recent period (417 m^3/s) about 9% greater than the earlier period (384 m^3/s). A comparison of the Upper Hudson alone for the two periods yields a similar increase of 12%, from 214 to 240 m^3/s.

Seasonally, the variations in MLW, MHW, and tidal range correspond with the variations in discharge (Figure 4). Generally, the tidal range decreases with increased river discharge due to increased frictional damping of the tide wave (Godin, 1991, 1999; Kukulka & Jay, 2003). At Albany before 1930, the average tidal range during the spring freshet was 0.4 m compared with about 0.9 m during summer low flow conditions (Figure 4b). In contrast, the mean water level (not shown) increased seasonally with discharge. The increase in MWL and reduction in tidal amplitude with discharge determines the seasonal cycle of MLW and MHW. During high flow, MLW increased due both to the increase in river discharge and the reduced tidal range (Figures 4c and 4d). By contrast, reduced tide range during high river flow tends to lower HW, counteracting to some extent the effect of increased MWL with the river discharge. Prior to 1930, both MLW and MHW increased on average by about 1 m during the spring freshet compared with the rest of the year. The seasonal correspondence of water level and discharge was much weaker for the period after 1980, with MHW varying seasonally by only ~0.4 m and MLW by less than 0.2 m. During the summer low discharge period, the average MHW in the modern estuary has increased by ~0.2 m and average MLW has decreased by 0.6 m compared to the predredging period. In addition to the seasonal variation in river discharge, damping of the tide by ice coverage (Georgas, 2011) also contributes to the annual variability. For example, in the modern estuary the annual minimum in tide range occurs prior to the maximum discharge during the spring freshet and instead during the winter months when ice coverage is a factor.

MWL, MHW, MLW, or any other tidal datum (TD) at Albany can be represented as a function of oceanic forcing, river flow, and frictional effects due to the tide:

$$TD_{Albany} = a_0 + \underbrace{a_1 * MSL_{Battery}(t)}_{SeaLeveleffect} + \underbrace{a_2 Q_r^b}_{RiverFlowEffect} + \underbrace{a_3 \frac{TR_{BATTERY}^2}{Q_r^n}}_{TideContribution} \tag{2}$$

where a_1, a_2, a_3, b, and n are empirically derived coefficients and a_0 is an offset to a geodetic datum (Jay et al., 2011; Kukulka & Jay, 2003). When river flow is large, it dominates and the effect of the tides is small or negligible. The relationship with discharge is often assumed to be linear, or $b = 1$, as is in the Columbia River (Kukulka & Jay, 2003). The similar long-term rates of MTL between The Battery and Albany increase suggests that a_1 is also close to 1 here. In the limit of low river flow, tidal forcing becomes increasingly important in setting the mean water level thru frictional effects and in setting MHW and MLW with an increasing tidal range.

Plotting MLW as a function Q_r, a distinct change in the relationship between water level at Albany and river discharge occurred around the time of dredging of the upper river in the late 1920s (Figure 5). For both the predredging and modern conditions the assumption is reasonable that the rating curve for MLW is approximately linear with discharge, or $b = 1$ in equation (2), but the two periods have distinctly different slopes. Before 1930, each additional 1,000 m^3/s of river flow increased MLW by 1.6 m, while in the modern estuary the corresponding increase in MLW was 0.9 m. At low discharge, MLW varied more with the tidal amplitude, but at higher discharges the tides were damped in the upper river and the dependence of water level on discharge was more direct. The change in water level with discharge reflects the fundamental result that the river slope for any given discharge has decreased over time, as explained below.
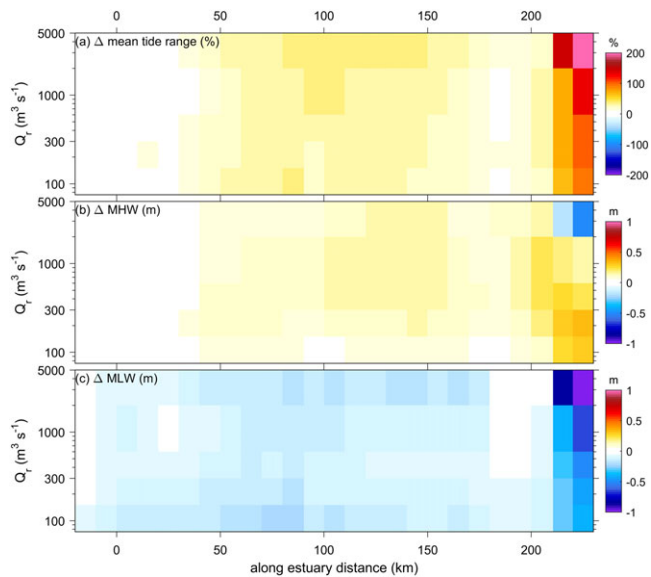
Figure 6. Modeled changes in the tide with distance along the estuary and as a function of discharge. (a) Relative change in mean tidal range between predredging and modern bathymetry, as a fraction of predredging range, (b) absolute difference in mean high water (MHW), and (c) absolute difference in mean low water (MLW).

The water level data indicate a weaker response of water level to discharge in the modern estuary (Figure 5), with changes in seasonal discharge patterns (Figure 4) and sea level rise as secondary factors (Figure 3). The tidally averaged momentum equation for the river can be reduced to a balance between pressure gradient and friction (Buschman et al., 2009; Hoitink & Jay, 2016), or

$$g\frac{\partial \eta}{\partial x} = \frac{C_d U^2}{H} \tag{3}$$

where $\partial \eta / \partial x$ is the water surface slope, C_d is a drag coefficient, U is the river velocity, and H is the water depth. In this balance, an increase in channel depth decreases the mean water surface slope for a given river discharge, lowering the water level at the landward end. Thus, the reduction in friction by dredging modifies the relationship between river flow and water level (equation (2)), as well as increasing tidal range (equation (1)). Tidal currents and the mean river flow effectively increase the drag due to the quadratic dependence and introduce asymmetries between MLW and MHW (Godin, 1999; Kukulka & Jay, 2003). Increased tidal range and velocity may enhance this frictional interaction, increasing the effective drag and partially offsetting the effect of increased depth. In the Hudson River, as also shown in the Columbia River (Jay et al., 2011) and in the Ems River (Jensen et al., 2003), the reduction in friction due to depth increases outweighed any increase in C_d. In the MLW observations from Albany, the change in slope was consistent with an inverse dependence on water depth in equation (3), although we note that changes in U may also contribute. The average depths in the upper 60 km increased from 3.7 to 6.3 m, similar to the ratio of the slopes of the linear relationships before and after dredging. For a discharge of 500 m³/s this corresponded with a reduction in water level of 0.8 m, whereas for high discharge event of 2,500 m³/s the difference in water level was 2.1 m. Similarly, analysis of water levels in the upper Columbia found that since 1902 mean water level dropped by 0.3–1.5 m, depending on discharge (Jay et al., 2011).

The response of the tide and mean water level to changes in depth with dredging varied with distance along the estuary. From the model, tidal amplitude on average increased moderately (20%–25%) over much of the lower estuary but was most pronounced in the upper 40 km of the tidal river, where tides more than doubled (Figure 6). At low discharge, MHW increased along the estuary because the tidal amplification effect was greater than the reduction in mean river slope. At high discharge, the reverse was true, as MHW decreased compared to the predredging case due to the increased hydraulic efficiency and decreased slope for the mean flow. The effects were additive for mean low water, such that water level decreased everywhere for low discharge, but the decreases were greatest in the upper tidal river during high discharge conditions (Figure 6).

3.3. Extreme Events

As with tides, channel deepening may reduce the damping of a surge wave produced at the ocean boundary (Familkhalili & Talke, 2016). Storm surge in the estuary also depends on its magnitude at the ocean boundary, and analysis of water level at The Battery from 1844 to 2013 suggests that storm surge amplitudes in New York Harbor are increasing faster than sea level rise (Talke et al., 2014). To assess directly how bathymetric changes have affected water level during extreme events, the model was run with both modern and predredging bathymetries for recent major storms: Hurricane Sandy in 2012 and Tropical Storms Irene and Lee in 2011 (Figure 7).

During Hurricane Sandy, the maximum water level at The Battery was about 3.4 m above MSL, 2.8 m greater than the predicted high tide and the largest storm surge tide (defined as total water level minus annual mean water level) since at least 1700 (Orton et al., 2016). The simulation with modern bathymetry produced a maximum water level during Sandy that was 0.5 m less than observed (Figure 7c), an underprediction similar to other simulations of the event (Orton et al., 2016). The underprediction may be due to errors in the water level at the open boundary or the wind field or in the parameterization of the surface friction coefficient. The same
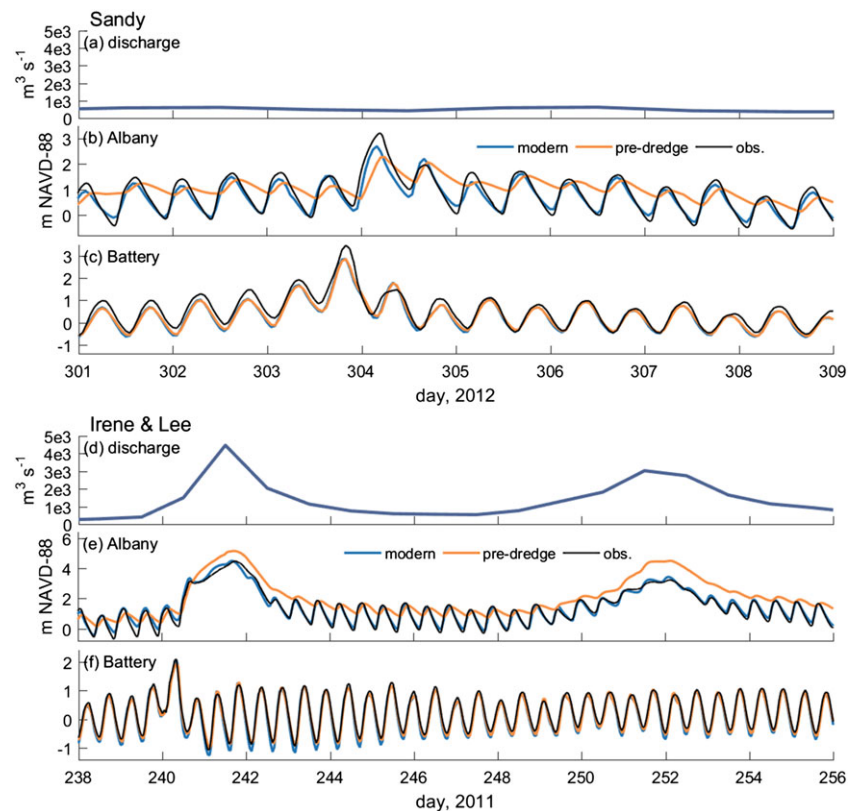
Figure 7. Discharge from the Upper Hudson and Mohawk Rivers (a, d) and water level at Albany (b, e) and The Battery (c, f) during and after major storm events, from observations and model results using predredging and modern bathymetries. (a–c) Hurricane Sandy in 2012 had a record coastal storm surge, while (d–f) Tropical Storms Irene and Lee in 2011 brought high river discharge.

forcing was used for both bathymetric configurations, and the results show that differences in water levels were small at The Battery between the modern and predredging bathymetry for the Hurricane Sandy cases. With the predredging bathymetry, the water level was a few centimeters lower at The Battery and the arrival was about 0.5 hr later than with the modern bathymetry. The change in storm surge was modest despite the large changes in channel depth near the mouth and is consistent with the observation that the change in tidal amplitude was also small. Analysis of water level records in back-barrier bays also showed that the storm surge response before and after Hurricane Sandy was unchanged despite large changes in inlet morphology (Aretxabaleta et al., 2014). The low-frequency variability and short propagation distance between the ocean and The Battery allows for little frictional transformation of the coastal setup. Moreover, Sandy was a relatively slow moving storm, such that the effects of altered depth on frictional damping were less pronounced than in a fast-moving storm (see Orton et al., 2015).

Model results showed a large change in the total water levels in the upper river for the storm surge of Sandy. The total water level (combining tides, meteorologically forced surge, and river flow) in the modern case was 0.4 m higher and 1.5 hr earlier than with the predredging bathymetry (Figure 7b). The 0.4-m increase in the maximum water level was a combination of competing effects—mean water level before the storm was lower with the modern bathymetry due to the reduction in river slope, but the predicted high tide was greater. Sandy brought little precipitation, so river discharge had a negligible effect on water level (Figure 7a). The differences between the model cases therefore reflect the reduction in friction, which allowed the surge wave to propagate up the tidal river with less dissipation than in the predredging bathymetry.

In contrast to Sandy, Tropical Storms Irene and Lee in 2011 produced extremely high river discharge but smaller storm surge. The combined discharge of the Upper Hudson and Mohawk was nearly 5,000 m³/s
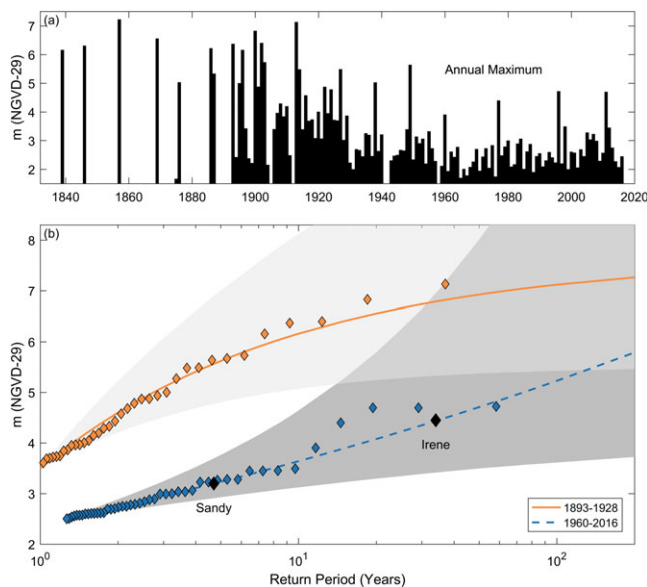
Figure 8. Observed flood frequency at Albany. (a) Annual maximum water level. (b) Water level return period based on a generalized Pareto distribution analysis of periods prior to dredging (1893–1928) and after (1960–2016). The shaded region gives the 95% confidence interval, and the diamond markers are unbiased return periods based on rank-ordered data (e.g., Makkonen, 2006). Observed maximum water levels during storms Irene (2011) and Sandy (2012) are noted for reference with black diamonds.

due to Irene, the second largest since 1918, and Lee followed 2 weeks later with over 3,000 m³/s (Figure 7d). As in the Sandy simulations, the effect of changing bathymetry on total water level (storm surge and tides) at The Battery due to Irene was negligible (Figure 7e). However, the effect of these storms on water levels in Albany was opposite that of Sandy, as water levels for Irene and Lee were 0.7 and 1.2 m *larger* with the historical grid than the modern (Figure 7f). During the peak of the Irene and Lee flood waves, the tidal range and coastal surge wave nearly disappeared, and water levels were primarily forced by river discharge. The increased hydraulic efficiency in the modern system was able to transport flood waters more effectively than the historic system, reducing extreme water levels. At The Battery, the discharge flood waves were more diffuse and the differences in water elevation were much smaller, with the tidally filtered water level in the predredging case about 10 cm higher than the modern case.

The model results therefore indicate that channel deepening has only marginally changed the total water level caused by storm surge and tides in New York Harbor but has significantly altered the response to storm events in the upper tidal river. When discharge is low, the reduction in effective drag with a deeper channel allows greater propagation of storm surge to Albany from the coast. However, the water level associated with a major storm surge event like Sandy remains far below the water level observed during both historical and modern river discharge events (Figure 8). When discharge is high, the tide and surge from the ocean are damped and the water level in the upper tidal river is primarily driven by the river slope. The more efficient conveyance of river flow after channel deepening has reduced the river slope, reducing water levels during discharge events.

The combined impact of channel deepening and flow regulation on flood hazard in Albany is quantified by calculating recurrence intervals for predredging (1888–1929) and modern (1977–2017) water level data (Figure 8). In both the time series of annual maximum and in the statistical model of exceedance probability, anthropogenic modification of the system has been concordant with a major reduction in the occurrence of high water events. The magnitudes of the 10 and 100-year recurrence interval events are now 2.6 and 2.0 m less, respectively, than historically. Moreover, the slope of the exceedance curve has been reduced, such that the difference between historical and modern water levels increases for smaller probability (longer return period) events. Historically, the 10-year event was more than 2 m above the annual event (6.2 m versus 3.9 m), compared with about 1-m difference in the modern system (3.6 m versus 2.5 m).

The changes in extreme water level recurrence depend on shifts in the river discharge patterns and the increase in channel depth. Several of the highest water level events historically were caused by ice dams during the spring melt (Schureman, 1934), but spring freshet flows have been reduced in recent decades compared to pre-1930 by flow regulation, climate change, and shifts in precipitation patterns (Figure 4). Before 1930, only two of the top 50 measured water levels (Schureman, 1934; our data) were due to hurricanes, whereas Irene, Lee, and Sandy brought three major tropical storm events in the past decade. This qualitative observation is consistent with an increase in the risk of compound flooding caused by combined storm surge and precipitation in the Eastern United States over the last century (Wahl et al., 2015). Hence, the increased relative importance of coastal storm events stems from a combination of the altered hydrograph, reduced river slope, and reduced damping of tides and storm surge.

The flooding event of record at Albany occurred in March 1913 due to excessive rainfall, snowmelt, and saturated or frozen ground, resulting in peak discharges in the Mohawk and Upper Hudson that exceeded the 100 year return period flood (Lumia & Murray, 1993). Extensive damage caused by the flooding spurred construction of the Conklingville Dam on the Upper Hudson, which became operational in 1930. To isolate the contributions of altered discharge and channel deepening on flooding, we calculate discharge recurrence
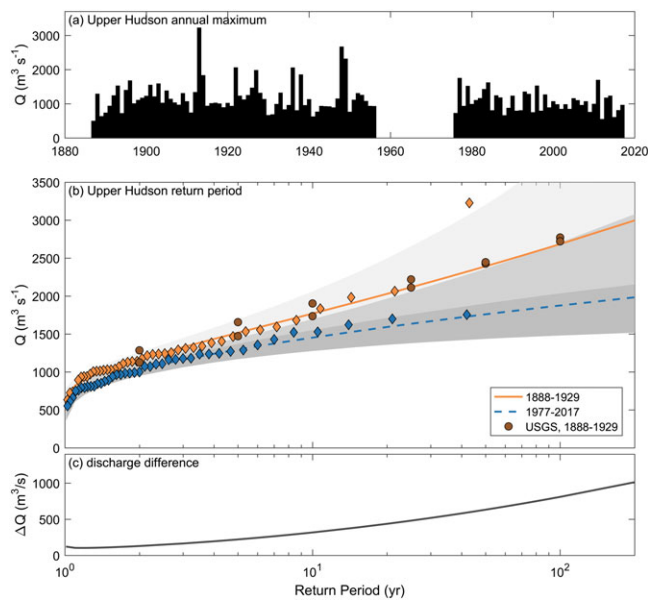
Figure 9. Observed discharge event frequency for the Upper Hudson at Waterford. (a) Annual maximum discharge. (b) Discharge return interval based on a Generalized Extreme Value distribution analysis of the period prior to major discharge regulation (1888–1929) and a similar time span recently (1977–2017). The diamond markers are unbiased return intervals based on rank-ordered data (e.g., Makkonen, 2006). Return intervals calculated by the USGS for the same data prior to discharge regulation but using log-Pearson type III and regional regression analyses (Lumia et al., 2006) are shown for reference.

intervals for the Upper Hudson before and after dam construction (Figure 9). A distinct difference in flow magnitudes is observed between the historical and modern periods. For the 10-year event, regulated flow in the Upper Hudson is now about 300 m^3/s less than prior to dam construction, and for the 100-year event the reduction is about 800 m^3/s. The calculated recurrence intervals were similar to previously published analyses of the predam discharge record (Lumia et al., 2006; Figure 9). Using the relationship between discharge and water level observed prior to 1930 of 1.6 m per 1,000 m^3/s (Figure 5), the decrease in flow for the 10-year event corresponded to a decrease in water level of 0.5 m, and the 100-year flow event water level decreased by 1.3 m. The total decreases in water level for the 10 and 100-year water levels at Albany (2.6 and 2.0 m, Figure 8) were greater than these decreases due to flow regime alone, indicating that the net reduction in flood risk is due both to flow regulation and channel deepening in the estuary.

4. Summary and Discussion

Our study investigates how channel deepening by dredging has altered the barotropic hydrodynamics of the Hudson River estuary over the past 150 years. Results show that the water level was most affected in the upper 40 km of the tidal river, which dredging transformed from a shallow, braided, island-filled river into a single, deeper channel (Collins & Miller, 2012). In this region tidal amplitude more than doubled and the landward conveyance of coastal storm surge increased, increasing the likelihood that annual maxima in water level are driven by marine processes. However, the overall risk of flooding has decreased for several reasons. During river discharge events water levels decreased due to the reduction in effective drag and the greater hydraulic conveyance caused by the deeper navigational channel, reducing the tidally averaged water surface slope between Albany and the ocean. The reduction in friction also produced an asymmetric response in the tidal water level, with mean low water decreasing more than the increase in mean high water. This introduces potential hazards for navigation, because increased depth due to dredging is offset by lower low water levels. The Columbia River had a similar response of decreasing low waters after dredging and potential impacts on navigation (Jay et al., 2011).

The amplification of tides and decreased mean water levels has ecological implications for estuarine and fluvial habitat. Mean water level changes in combination with seasonal changes in the hydrograph alter wetland inundation patterns and influence ecological zonation (Jay et al., 2015). The decrease in extreme water levels means that some elevations that formerly were inundated occasionally are rarely or never under water today. The type of inundation has also changed. Whereas inundation formerly occurred over long periods in early spring due to seasonal river flow, inundation today is more likely to be episodic due to the amplified tides and storm surge from the ocean. While major changes to the barotropic dynamics and flood hazard in the upper Hudson have been driven by channel modifications and altered river flow, our results suggest an increasing effect of sea level rise on mean water level over the past 50 years more than 250 km from the coast (Figure 3). Recent estimates suggest that sea level in New York Harbor will rise 0.73 m (range of 0.28 to 1.32 m) by the year 2100 using the *business as usual* RCP 4.5 scenario (Kopp et al., 2017). Our results suggest that an increase in mean water level of this magnitude, while still small compared to the historical doubling of depth near Albany, is large enough to further amplify tides and storm surge magnitudes in the upper Hudson, while reducing river slope (see also Orton et al., 2018).

References

Abood, K. A. (1974). Circulation in the Hudson Estuary. *Annals of the New York Academy of Sciences*, *250*(1), 39–111. https://doi.org/10.1111/j.1749-6632.1974.tb43895.x

Amin, M. (1983). On perturbations of harmonic constants in the Thames Estuary. *Geophysical Journal International*, *73*(3), 587–603. https://doi.org/10.1111/j.1365-246X.1983.tb03334.x

Aretxabaleta, A. L., Butman, B., & Ganju, N. K. (2014). Water level response in back-barrier bays unchanged following Hurricane Sandy. *Geophysical Research Letters*, *41*, 3163–3171. https://doi.org/10.1002/2014GL059957

Bowen, M. M., & Geyer, W. R. (2003). Salt transport and the time-dependent salt balance of a partially stratified estuary. *Journal of Geophysical Research*, *108*(C5), 3158. https://doi.org/10.1029/2001JC001231

Burchard, H., Schuttelaars, H. M., & Ralston, D. K. (2018). Sediment trapping in estuaries. *Annual Review of Marine Science*, *10*(1), 371–395. https://doi.org/10.1146/annurev-marine-010816-060535

Buschman, F. A., Hoitink, A. J. F., van der Vegt, M., & Hoekstra, P. (2009). Subtidal water level variation controlled by river flow and tides. *Water Resources Research*, *45*, W10420. https://doi.org/10.1029/2009WR008167

Cai, H., Savenije, H. H. G., Yang, Q., Suying, O., & Yaping, L. (2012). Influence of river discharge and dredging on tidal wave propagation: Modaomen Estuary case. *Journal of Hydraulic Engineering*, *138*(10), 885–896. https://doi.org/10.1061/(ASCE)HY.1943-7900.0000594

Chant, R. J., Sommerfield, C. K., & Talke, S. A. (2018). Impact of channel deepening on tidal and gravitational circulation in a highly engineered Estuarine Basin. *Estuaries and Coasts*, *41*(6), 1587–1600. https://doi.org/10.1007/s12237-018-0379-6

Collins, M. J., & Miller, D. (2012). Upper Hudson River Estuary (USA) floodplain change over the 20th century. *River Research and Applications*, *28*(8), 1246–1253. https://doi.org/10.1002/rra.1509

de Jonge, V. N., Schuttelaars, H. M., van Beusekom, J. E. E., Talke, S. A., & de Swart, H. E. (2014). The influence of channel deepening on estuarine turbidity levels and dynamics, as exemplified by the Ems estuary. *Estuarine, Coastal and Shelf Science*, *139*, 46–59. https://doi.org/10.1016/j.ecss.2013.12.030

DiLorenzo, J. L., Huang, P., Thatcher, M. L., & Najarian, T. O. (1993). Dredging impacts of Delaware estuary tides. In *Proc. 3rd Int. Conf. Sponsored by the Waterway, Port, Coastal and Ocean Division, ASCE* (pp. 86–104). Oak Brook, IL.

Familkhalili, R., & Talke, S. A. (2016). The effect of channel deepening on tides and storm surge: A case study of Wilmington, NC. *Geophysical Research Letters*, *43*, 9138–9147. https://doi.org/10.1002/2016GL069494

Flick, R. E., Murray, J. F., & Ewing, L. C. (2003). Trends in United States tidal datum statistics and tide range. *Journal of Waterway, Port, Coastal, and Ocean Engineering*, *129*(4), 155–164. https://doi.org/10.1061/(ASCE)0733-950X(2003)129:4(155)

Friedrichs, C. T. (2010). Barotropic tides in channelized estuaries. In *Contemporary issues in estuarine physics* (pp. 27–61). https://doi.org/10.1017/CBO9780511676567.004

Friedrichs, C. T., & Aubrey, D. G. (1994). Tidal propagation in strongly convergent channels. *Journal of Geophysical Research*, *99*(C2), 3321–3336. https://doi.org/10.1029/93JC03219

Georgas, N. (2011). Large seasonal modulation of tides due to ice cover friction in a midlatitude estuary. *Journal of Physical Oceanography*, *42*(3), 352–369. https://doi.org/10.1175/JPO-D-11-063.1

Godin, G. (1991). Frictional effects in river tides. In B. Parker (Ed.), *Progress in tidal hydrodynamics* (pp. 379–402). New York: John Wiley.

Godin, G. (1999). The propagation of tides up rivers with special considerations on the Upper Saint Lawrence River. *Estuarine, Coastal and Shelf Science*, *48*(3), 307–324. https://doi.org/10.1006/ecss.1998.0422

Haidvogel, D. B., Arango, H., Budgell, W. P., Cornuelle, B. D., Curchitser, E., di Lorenzo, E., Fennel, K., et al. (2008). Ocean forecasting in terrain-following coordinates: Formulation and skill assessment of the Regional Ocean Modeling System. *Journal of Computational Physics*, *227*(7), 3595–3624. https://doi.org/10.1016/j.jcp.2007.06.016

Hayhoe, K., Wake, C. P., Huntington, T. G., Luo, L., Schwartz, M. D., Sheffield, J., Wood, E., et al. (2007). Past and future changes in climate and hydrological indicators in the US Northeast. *Climate Dynamics*, *28*(4), 381–407. https://doi.org/10.1007/s00382-006-0187-8

Hoitink, A. J. F., & Jay, D. A. (2016). Tidal river dynamics: Implications for deltas. *Reviews of Geophysics*, *54*, 240–272. https://doi.org/10.1002/2015RG000507

Jalón-Rojas, I., Schmidt, S., Sottolichio, A., & Bertier, C. (2016). Tracking the turbidity maximum zone in the Loire Estuary (France) based on a long-term, high-resolution and high-frequency monitoring network. *Continental Shelf Research*, *117*, 1–11. https://doi.org/10.1016/j.csr.2016.01.017

Jalón-Rojas, I., Sottolichio, A., Hanquiez, V., Fort, A., & Schmidt, S. (2018). To what extent multidecadal changes in morphology and fluvial discharge impact tide in a convergent (turbid) tidal river. *Journal of Geophysical Research: Oceans*, *123*, 3241–3258. https://doi.org/10.1002/2017JC013466

Jay, D. A. (1991). Green's law revisited: Tidal long-wave propagation in channels with strong topography. *Journal of Geophysical Research*, *96*(C11), 20,585–20,598. https://doi.org/10.1029/91JC01633

Jay, D. A., Leffler, K., & Degens, S. (2011). Long-term evolution of Columbia River tides. *Journal of Waterway, Port, Coastal, and Ocean Engineering*, *137*(4), 182–191. https://doi.org/10.1061/(ASCE)WW.1943-5460.0000082

Jay, D. A., Leffler, K., Diefenderfer, H. L., & Borde, A. B. (2015). Tidal-fluvial and estuarine processes in the lower Columbia River: I. Along-channel water level variations, Pacific Ocean to Bonneville Dam. *Estuaries and Coasts*, *38*(2), 415–433. https://doi.org/10.1007/s12237-014-9819-0

Jensen, J., Mudersbach, C., & Blasi, C. (2003). Hydrological changes in tidal estuaries due to natural and anthropogenic effects. In *6th International MEDCOAST 2003 Conference*. Ravenna, Italy.

Klingbeil, A. D., & Sommerfield, C. K. (2005). Latest Holocene evolution and human disturbance of a channel segment in the Hudson River Estuary. *Marine Geology*, *218*(1–4), 135–153. https://doi.org/10.1016/j.margeo.2005.02.026

Kopp, R. E., DeConto, R. M., Bader, D. A., Hay, C. C., Horton, R. M., Kulp, S., Oppenheimer, M., et al. (2017). Evolving understanding of Antarctic ice-sheet physics and ambiguity in probabilistic sea-level projections. *Earth's Future*, *5*(12), 1217–1233. https://doi.org/10.1002/2017EF000663

Kotz, S., & Nadarajah, S. (2000). *Extreme value distributions: Theory and applications*. London: Imperial College Press, World Scientific. https://doi.org/10.1142/p191

Kukulka, T., & Jay, D. A. (2003). Impacts of Columbia River discharge on salmonid habitat: 1. A nonstationary fluvial tide model. *Journal of Geophysical Research*, *108*(C9), 3293. https://doi.org/10.1029/2002JC001382

Lumia, R., Freehafer, D. A., & Smith, M. J. (2006). Magnitude and frequency of floods in New York. U.S. Geological Survey.

Lumia, R., & Murray, P. M. (1993). Maximum known stages and discharges of New York streams, 1865-1989, with descriptions of five selected floods, 1913-85 (Water-Resources Investigation Report No. 92–4042) (p. 123). Albany, New York: U.S. Geological Survey.

Makkonen, L. (2006). Plotting positions in extreme value analysis. *Journal of Applied Meteorology and Climatology*, *45*(2), 334–340. https://doi.org/10.1175/JAM2349.1

Marmer, H. A. (1935). *Tides and currents in New York Harbor* (Vol. 4). Washington, DC: U.S. Government Printing Office.

Nichols, M. M., & Biggs, R. B. (1985). Estuaries. In R. A. Davis (Ed.), *Coastal Sedimentary Environments* (pp. 77–186). New York: Springer.

Orton, P. M., Conticello, F. R., Cioffi, F., Hall, T. M., Georgas, N., Lall, U., Blumberg, A. F., et al. (2018). Flood hazard assessment from storm tides, rain and sea level rise for a tidal river estuary. *Natural Hazards*. https://doi.org/10.1007/s11069-018-3251-x

Orton, P. M., Hall, T. M., Talke, S. A., Blumberg, A. F., Georgas, N., & Vinogradov, S. (2016). A validated tropical-extratropical flood hazard assessment for New York Harbor. *Journal of Geophysical Research: Oceans*, *121*, 8904–8929. https://doi.org/10.1002/2016JC011679

Orton, P. M., Talke, S. A., Jay, D. A., Yin, L., Blumberg, A. F., Georgas, N., et al. (2015). Channel shallowing as mitigation of coastal flooding. *Journal of Marine Science and Engineering*, *3*(3), 654–673.

Panuzio, F. L. (1965). Lower Hudson River siltation. In *Proceedings of the 2nd Federal Interagency Sedimentation Conference* (pp. 512–550). Jackson, MS: Agricultural Research Service.

Ralston, D. K., & Geyer, W. R. (2018). Sediment transport time scales and trapping efficiency in a tidal river. *Journal of Geophysical Research: Earth Surface*, *122*, 2042–2063. https://doi.org/10.1002/2017JF004337

Ralston, D. K., Geyer, W. R., & Lerczak, J. A. (2008). Subtidal salinity and velocity in the Hudson River Estuary: Observations and modeling. *Journal of Physical Oceanography*, *38*(4), 753–770. https://doi.org/10.1175/2007JPO3808.1

Ralston, D. K., Geyer, W. R., & Warner, J. C. (2012). Bathymetric controls on sediment transport in the Hudson River estuary: Lateral asymmetry and frontal trapping. *Journal of Geophysical Research*, *117*, C10013. https://doi.org/10.1029/2012JC008124

Ralston, D. K., Warner, J. C., Geyer, W. R., & Wall, G. R. (2013). Sediment transport due to extreme events: The Hudson River estuary after tropical storms Irene and Lee. *Geophysical Research Letters*, *40*, 5451–5455. https://doi.org/10.1002/2013GL057906

Schureman, P. (1934). *Tides and currents in Hudson River* (Vol. 180). Washington, DC: United States Government Printing Office.

Steinberg, T. (2014). *Gotham unbound: The ecological history of greater*. New York: Simon and Schuster.

Talke, S. A., de Swart, H. E., & De Jonge, V. N. (2009). An idealized model and systematic process study of oxygen depletion in highly turbid estuaries. *Estuaries and Coasts*, *32*(4), 602–620. https://doi.org/10.1007/s12237-009-9171-y

Talke, S. A., de Swart, H. E., & Schuttelaars, H. M. (2009). Feedback between residual circulations and sediment distribution in highly turbid estuaries: An analytical model. *Continental Shelf Research*, *29*(1), 119–135. https://doi.org/10.1016/j.csr.2007.09.002

Talke, S. A., & Jay, D. A. (2013). Nineteenth century North American and Pacific tidal data: Lost or just forgotten? *Journal of Coastal Research*, *29*(6a), 118–127.

Talke, S. A., & Jay, D. A. (2017). Archival water-level measurements: Recovering historical data to help design for the future. In *Civil and Environmental Engineering Faculty Publications and Presentations 412*. Retrieved from https://pdxscholar.library.pdx.edu/cengin_fac/412

Talke, S. A., Orton, P., & Jay, D. A. (2014). Increasing storm tides in New York Harbor, 1844–2013. *Geophysical Research Letters*, *41*, 3149–3155. https://doi.org/10.1002/2014GL059574

Vellinga, N. E., Hoitink, A. J. F., van der Vegt, M., Zhang, W., & Hoekstra, P. (2014). Human impacts on tides overwhelm the effect of sea level rise on extreme water levels in the Rhine–Meuse delta. *Coastal Engineering*, *90*(Supplement C), 40–50. https://doi.org/10.1016/j.coastaleng.2014.04.005

Wahl, T., Jain, S., Bender, J., Meyers, S. D., & Luther, M. E. (2015). Increasing risk of compound flooding from storm surge and rainfall for major US cities. *Nature Climate Change*, *5*(12), 1093–1097. https://doi.org/10.1038/nclimate2736

Wall, G., Nystrom, E., & Litten, S. (2008). Suspended sediment transport in the freshwater reach of the Hudson River Estuary in eastern New York. *Estuaries and Coasts*, *31*(3), 542–553. https://doi.org/10.1007/s12237-008-9050-y

Warner, J. C., Armstrong, B., He, R., & Zambon, J. B. (2010). Development of a Coupled Ocean–Atmosphere–Wave–Sediment Transport (COAWST) modeling system. *Ocean Modelling*, *35*(3), 230–244. https://doi.org/10.1016/j.ocemod.2010.07.010

Winterwerp, J. C. (2011). Fine sediment transport by tidal asymmetry in the high-concentrated Ems River: Indications for a regime shift in response to channel deepening. *Ocean Dynamics*, *61*(2-3), 203–215. https://doi.org/10.1007/s10236-010-0332-0

Winterwerp, J. C., Wang, Z. B., van Braeckel, A., van Holland, G., & Kösters, F. (2013). Man-induced regime shifts in small estuaries—II: A comparison of rivers. *Ocean Dynamics*, *63*(11–12), 1293–1306. https://doi.org/10.1007/s10236-013-0663-8